

RESEARCH LETTER

10.1029/2018GL079563

Key Points:

- Large-domain convective-permitting regional climate simulations can overcome bias in parent model
- Such a model run for 10 years over Africa shows stronger local Hadley overturning into the subtropics
- This improves the annual cycle of rainfall systems and reduces wet bias over subtropical southern Africa

Correspondence to:

N. C. G. Hart,
neil.hart@ouce.ox.ac.uk

Citation:

Hart, N. C. G., Washington, R., & Stratton, R. A. (2018). Stronger local overturning in convective-permitting regional climate model improves simulation of the subtropical annual cycle. *Geophysical Research Letters*, *45*, 11,334–11,342. <https://doi.org/10.1029/2018GL079563>

Received 10 JUL 2018

Accepted 5 OCT 2018

Accepted article online 9 OCT 2018

Published online 23 OCT 2018

Stronger Local Overturning in Convective-Permitting Regional Climate Model Improves Simulation of the Subtropical Annual Cycle

Neil C. G. Hart¹ , Richard Washington¹, and Rachel A. Stratton²

¹School of Geography and the Environment, University of Oxford, Oxford, UK, ²Met Office, Exeter, UK

Abstract Global climate models fail to represent the annual cycle of tropical-extratropical cloud bands and produce too much summer rainfall over subtropical southern Africa. This study demonstrates that running a regional convective-permitting climate simulation alleviates these biases, counteracting biases that are present in the parent model. The improvement emerges from stronger vertical mass flux in the tropics, which forces a stronger local Hadley overturning into the summer hemisphere. This enhanced overturning increases upper-level subsidence in the subtropics and amplifies the forcing of the local subtropical jet. Together, these improvements halve the wet subtropical rainfall bias and are associated with a 50% increase to an 80% match between the simulated and observed annual cycle of crucial tropical-extratropical cloud band rainfall systems. The results advocate for the increased use of convective-permitting climate models with domains that include regional tropical convection hot spots, in order to fully benefit from the explicit representation of deep convection.

Plain Language Summary Climate models, both global and regional, approximate the development and effect of thunderstorms on the simulated circulation. The inadequacy of these approximations is widely thought to produce inaccuracies in simulated regional climates. These errors are particularly severe over southern Africa where model simulations produce too much rain and poorly represent the annual cycle of the dominant summer rainfall systems. In this study, a pan-African regional climate simulation is run for 10 years at a grid spacing that allows direct simulation of widespread outbreaks of thunderstorms, breaking the model dependence on inadequate approximations. This *convection-permitting* model produces a substantially more realistic regional climate over subtropical southern Africa with the main rainfall systems occurring at the right time of year and only a moderate overestimate of monthly summer rainfall. This result is particularly striking because this regional model overcomes errors that are present in the global model which provides the boundary conditions to its pan-African domain.

1. Introduction

Convective-permitting climate simulations are revolutionizing our ability to quantify the role of mesoscale processes in regional hydroclimates. To date, this step change has been exemplified through the vastly improved representation of subdaily rainfall rates due to the simulation of mesoscale convection (Prein, Liu, Ikeda, Bullock, et al., 2017a; Stratton et al., 2018). This step change has resulted in more realistic simulation of current and future rainfall extremes at kilometer scales (Kendon et al., 2014, 2017; Prein, Liu, Ikeda, Trier, et al., 2017b). These studies have demonstrated that the improvements arise from the explicit simulation of convection organized across multikilometer scales; these models do not yet have the resolution necessary to resolve isolated convective cells. Few studies have considered how these resolved mesoscale processes have an upscale impact on regional climates. In this study, we analyze how such upscale processes can reduce subtropical rainfall biases and fix the annual cycle errors that plague Coupled Model Intercomparison Project Phase 5 (CMIP5) models over southern Africa.

Regional climate simulation errors in global models are substantial with 7 out of 10 CMIP5 models overestimating the rainfall by 150–200% over southern Africa in austral summer (Lazenby et al., 2016; Munday & Washington, 2017). This warm season rainfall is dominated by tropical-extratropical (TE) cloudbands, which manifest in the subtropics during synoptic-scale TE interactions known regionally as tropical temperature

troughs or TTTs (Harrison, 1984; Hart et al., 2013; Washington & Todd, 1999). Correct simulation of the seasonal cycle of TE cloudbands is therefore a first-order requirement if the rainfall climatology of climate models is to be useful. This seasonality is a challenge for climate models as it requires adequate representation of subdaily subtropical convection and a weakly forced subtropical jet over southern Africa (Hart et al., 2018). The simulated annual cycle of TE cloud bands in CMIP5 models is generally too flat without the dominant summertime peak in occurrence, a failing found in the Met Office Unified Model (UM), too (James et al., 2018).

In this study, we run a set of model experiments using a suite of configurations of the UM which demonstrate that these errors are alleviated when convection is represented explicitly.

2. Data and Methods

We use three model simulations: one global model and two pan-African limited area model (LAM) simulations all based on the UM physics (Brown et al., 2012). The global simulation is a 30-year run of the UM Global Atmosphere 7.0 (GA7) at N512 resolution ($\sim 26 \text{ km} \times 39 \text{ km}$ over Africa) with 85 vertical levels up to 85 km forced by daily sea surface temperatures from a 0.25° spatial grid. The first LAM (LAM25) was also configured at the N512 resolution of the global model ($\Delta x \sim 25 \text{ km}$) in a pan-African domain (39°N – 45°S , 25°W – 56°E) with 63 vertical levels and convective parametrization enabled. LAM25 also shares the same soil type specification as the second LAM, which improves comparability between LAMs. The second LAM (LAM4) featured a horizontal grid spacing of 4.5 km with the same domain as LAM25 and 80 levels up to 38.5 km. Convective parametrization was turned off. The LAMs were driven by 3-hourly lateral boundary conditions from the global model for 10 years and by observed sea and lake surface temperatures. See Stratton et al. (2018) for full details of the experiments.

TE cloud bands are identified from the extensively applied (Hart et al., 2013; Hart et al., 2018) object-based metbot algorithm (Hart et al., 2012). The method flags TE events on individual or consecutive days when low daily mean outgoing longwave radiation (OLR) extends in a northwest-southeast band from 20° to 40°S . The OLR threshold is based on the bimodal frequency distribution of subtropical OLR which features a low-valued peak for the deep cloud regions and a high-valued peak from the clear skies over the subtropical high pressure systems. In the UM simulations, 245 W/m^2 corresponds to the value in the saddle between these peaks and is used as the low-OLR threshold in this study. Sensitivity tests confirm that this remains an appropriate threshold for both the parametrized convection and convection-permitting simulations. The results presented here are insensitive to small (5 W/m) variations in this threshold, with, for example, the r^2 values reported in Figure 1 varying by less than 0.05 for such variations. The satellite-derived daily mean OLR estimates typically exhibit a value of 240 W/m^2 . Observed daily mean OLR is obtained from the interpolated National Oceanic and Atmospheric Administration Climate Data Record for 1979 to 2012, available on a $1^\circ \times 1^\circ$ grid (Lee, 2014). The model daily mean OLR is regridded onto the observational data grid before applying the metbot algorithm. The Tropical Rainfall Measuring Mission 3B42 satellite-estimated daily rainfall (TRMM; Huffman et al., 2007) is attributed to TE cloud bands when detected within the contours of a cloud band object, which provides a baseline estimate of the contribution of cloud bands, and, by inversion, noncloudband rainfall to the monthly rainfall totals.

3. Improvements in Simulated TE Cloud Band and Rainfall Seasonality

The observed annual cycle of TE cloud bands features a peak in the austral summer months from November to January inclusive and a negligible count in June to August inclusive (Hart et al., 2013). The global and regional convective-parametrized simulations underestimate cloud band frequency from January to April but overestimate winter (June to August) occurrence (Figures 1a and 1b), an error very similar to fully coupled climate versions of the UM (James et al., 2018). However, the seasonality simulated by the convection-permitting LAM4 model matches the observations more closely (Figure 1c), reflecting an improved r^2 value computed from the observed and simulated median seasonal cycle from 0.1 in the global model and 0.5 in LAM25 regional model to 0.8 in the convection-permitting model (LAM4).

Global and regional models tend to simulate a positive rainfall bias over southern Africa (Munday & Washington, 2017), and this is true also of the UM suit of models analyzed here. The annual cumulative bias for the global, LAM25, and LAM4 is 251, 317, and 142 mm, respectively, reflecting an improvement in the case of LAM4 (Figure 2). This subtropical area-averaged bias (area box depicted in Figures 2d–2f) improvement is associated with negligible change in biases across tropical Africa (Figures 2d–2f), apart from an increase

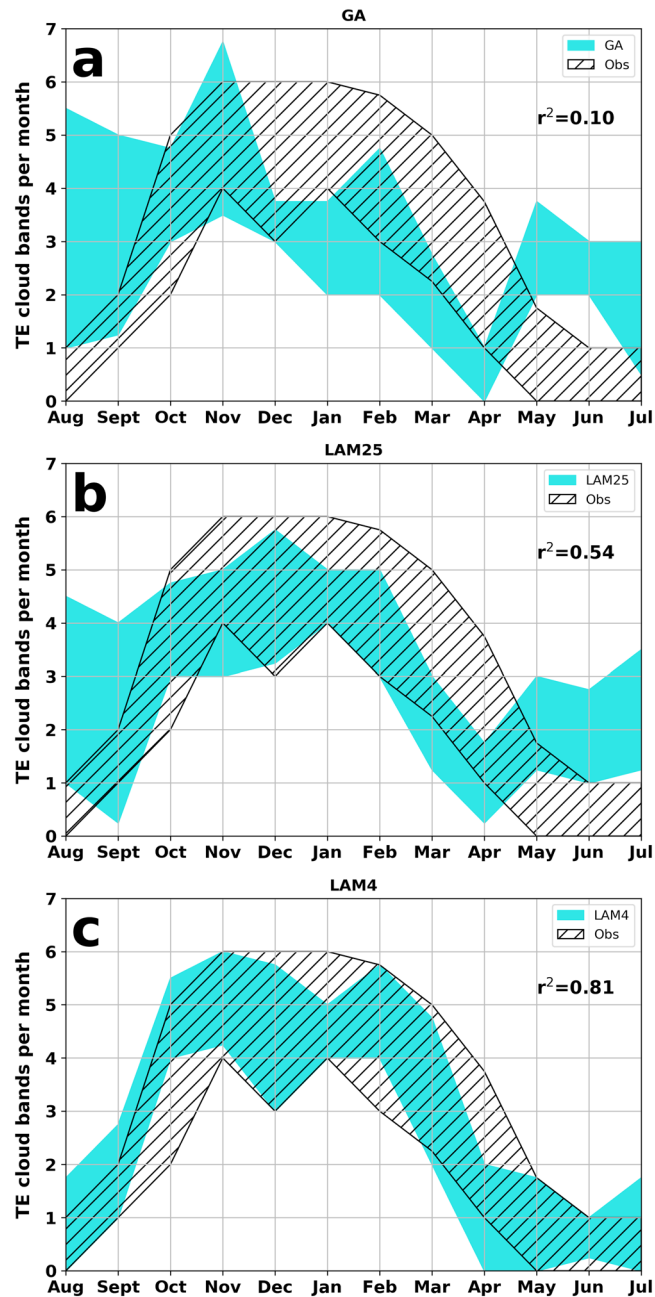


Figure 1. Seasonal cycle in the simulated interquartile range of monthly TE cloud band frequency over southern Africa by (a) GA N512, (b) regional LAM25, and (c) regional convective-permitting LAM4. The observed interquartile range is hatched for reference on each panel. Correspondence between the median seasonal cycle in cloud band count of the simulation and observations is shown by the r^2 value on each panel. GA = Global Atmosphere; LAM = limited area model; TE = tropical-extratropical.

in bias of 10–20% in a band across 10°–15°S. The reduction in subtropical model bias could be expected to derive partly from the simulation of rainfall from cloud bands, particularly given the primacy of these systems in the rainfall climatology of southern Africa and the improvement of the annual cycle of cloud band frequency in the LAM4. Cloud band rainfall error in the global, LAM25, and LAM4 is 71, 80, and 59 mm, respectively. This represents a small error reduction in LAM4 cloud band rainfall contributions compared with both parametrized convection models; most of the bias reduction comes from noncloudband rainfall.

Much of the improvement evident in LAM4 derives from early summer when the LAM4 simulated rainfall bias drops below 20 mm. This bias reduction occurs across much of southern Africa with the exception of

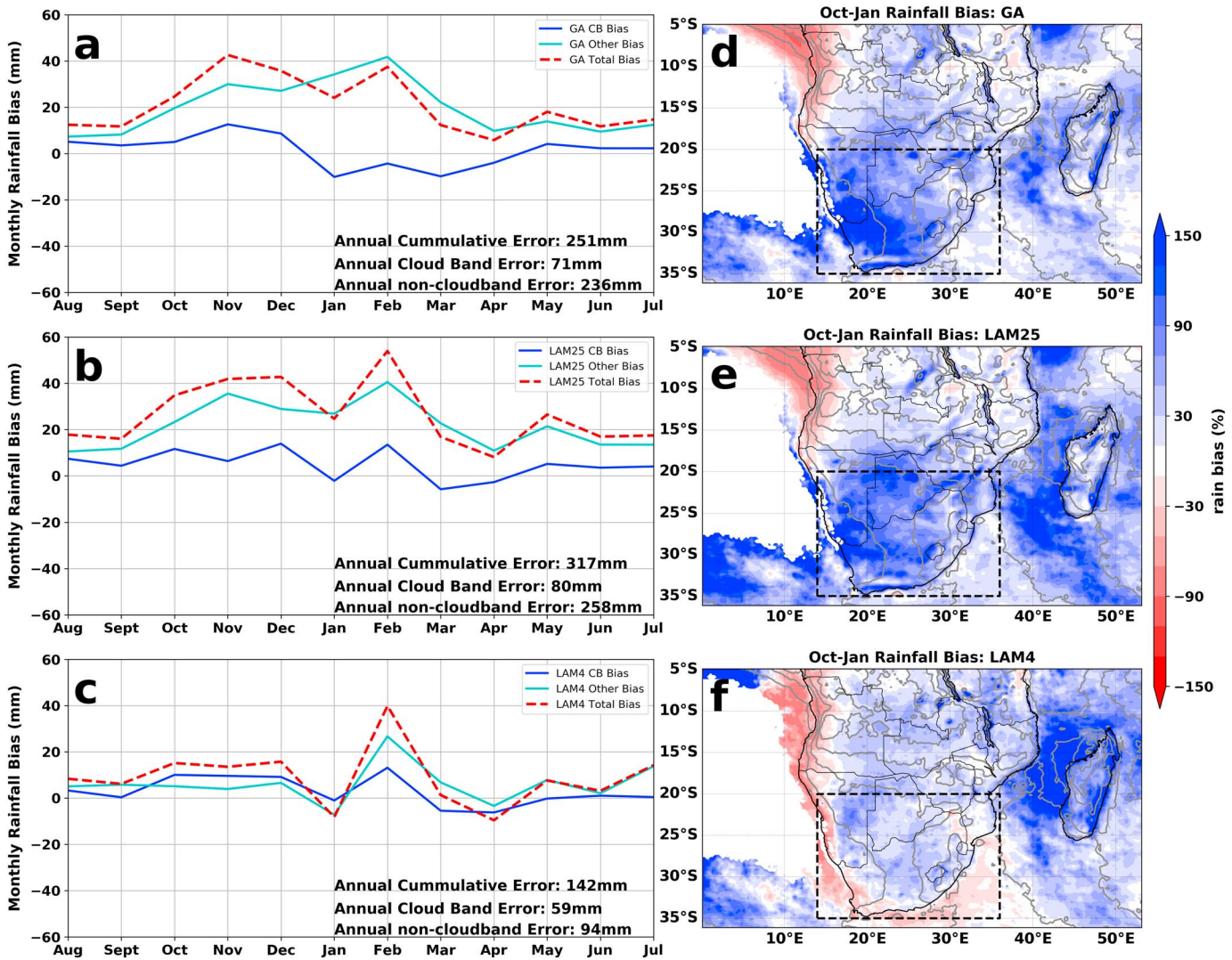


Figure 2. Monthly area-averaged (14°E–36°E, 20°E–35°S) rainfall bias with respect to TRMM rainfall observations simulated by (a) GA N512, (b) regional LAM25, and (c) regional convective-permitting LAM4. Total bias (red dashed) is decomposed into bias due to TE cloud band rainfall (dark blue) and bias due to rainfall from other systems (cyan). The accumulated annual error (sum of monthly absolute error) is given in the panel text for each of the simulations. Maps of total bias (% of climatological rainfall) in October to January rainfall simulated by (d) GA N512, (e) regional LAM25, and (f) regional convective-permitting LAM4. Domain for area averages in a–c indicated in black dashed box. Areas with annual rainfall <10 mm are masked. GA = Global Atmosphere; LAM = limited area model; TRMM = Tropical Rainfall Measuring Mission; TE = tropical-extratropical.

the high mountains near Lesotho (30°S; 30°E, Figures 2d–2f). LAM4 accurately simulates the dryness along the west coast of southern Africa which is poorly captured in both versions of the model with convective parametrization. In February, however, CP4 develops a large wet rainfall bias. This bias is most likely related to an overly strong coupling between convection and regional low-level convergence over the Mozambique Channel. Hints of this bias are seen in the October–January bias (Figures 2f), but the error is amplified in February across the northeastern parts of the subtropical domain since this is the peak month for convective instability in the region (Hart et al., 2018).

We have shown that the convection-permitting regional configuration, LAM4, is able to simulate an improved annual cycle of cloud bands and October–January rainfall more accurately than the global and LAM25 simulation. These improvements happen despite boundary forcing derived from the global model which simulates substantial regional errors suggesting that forcing which is internal to the LAM domain is associated with the improved fidelity of the LAM4 simulation. Next, we diagnose the common element of regional circulation that is associated with both of these improvements in LAM4.

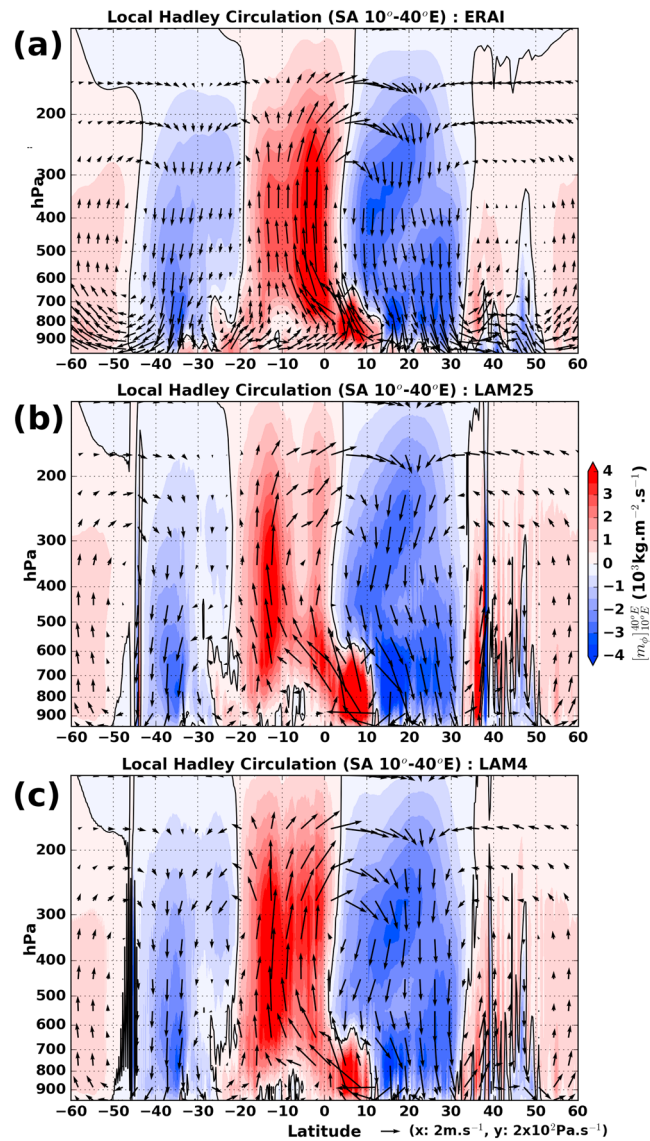


Figure 3. Local Hadley circulation depicted by meridional mass flux (shaded) for (a) ERAI, (b) LAM25, and (c) LAM4, averaged zonally across southern Africa (10°E to 40°E). Vectors show zonally averaged overturning circulation depicted by u_ϕ and w_ϕ (scaled by 2×10^2). ERAI = ERA-Interim; LAM = limited area model.

4. Strengthened Local Overturning Circulation

The tropospheric heating and upward mass flux associated with deep tropical convection, such as over tropical Africa, has a profound impact on subtropical climates. The associated divergent upper-level flow advects planetary vorticity poleward which supports a subtropical jet (Sardeshmukh & Hoskins, 1988). The subsidence of this divergent flow is manifested over southern African in the Botswana High (Reason, 2016). The structure of this mean state, particularly the presence of a subtropical jet, is fundamental to the frequent formation of TE cloud bands over southern Africa (Hart et al., 2018). Both the poleward divergent flow and the subtropical subsidence are part of local Hadley overturning which we now diagnose in the LAM25 and LAM4 simulations.

To calculate the simulated overturning, the vertical mass flux is decomposed into meridional and zonal components. For full details see the derivation developed by Schwendike et al. (2014). The decomposition is achieved by specifying a potential function μ related to velocity potential χ such that $\chi = \frac{\partial \mu}{\partial p}$, which when combined with the continuity equation yields

$$\nabla_p^2 \mu = -\omega \quad (1)$$

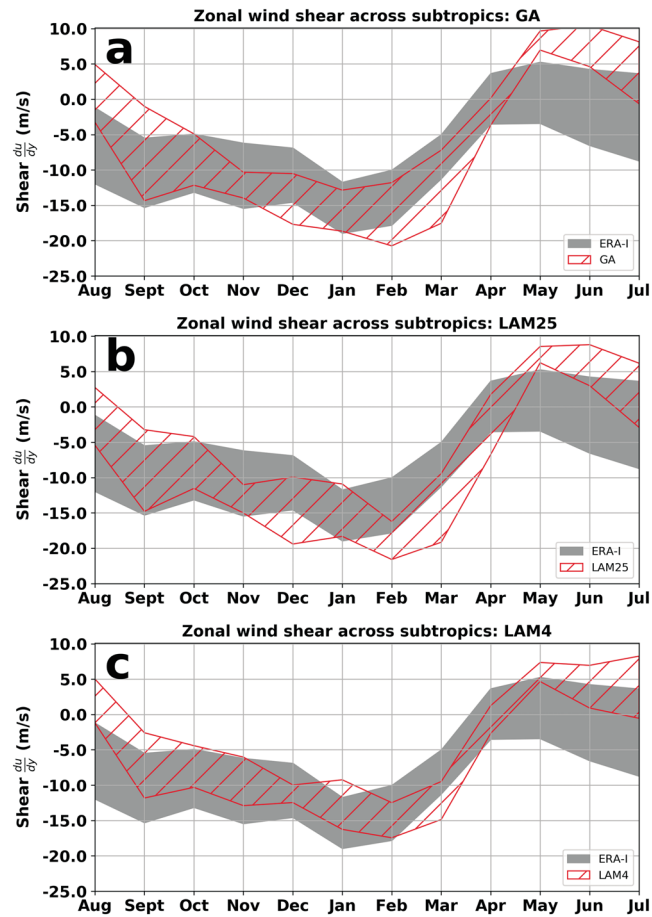


Figure 4. Interquartile range of shear in 250-mbar upper-level monthly mean zonal flow over subtropical southern Africa as simulated by (a) GA N512, (b) regional LAM25, and (c) regional convective-permitting LAM4. Interquartile range of ERAI is shown in gray shading with model-simulated interquartile range in red hatching. Shear computed as difference between mean zonal flow in 20°S–25°S band and 30°S–35°S bands. GA = Global Atmosphere; LAM = limited area model; ERAI = ERA-Interim.

where ω is vertical velocity. This equation is solved on the sphere, and to achieve this the LAM simulation data are spliced back into the global parent model data. Edge effects of this splice are small and do not affect the results presented here. By specifying the vector stream function $\psi = -\nabla_p \omega$, equation (1) can be rewritten as $\nabla_p \cdot \psi = \omega$. The zonal (λ) and meridional (ϕ) components of the three-dimensional flow can be computed from the relation of μ to χ , the definition of ψ , and since $\mathbf{u}_{\text{div}} = \nabla_p \chi$, which gives

$$(u_\lambda, u_\phi) = -\left(\frac{\partial \psi_\lambda}{\partial p}, \frac{\partial \psi_\phi}{\partial p}\right) \quad ; \quad (\omega_\lambda, \omega_\phi) = \left(\frac{1}{a \cos \phi} \frac{\partial \psi_\lambda}{\partial \lambda}, \frac{1}{a \cos \phi} \frac{\partial \psi_\phi \cos \phi}{\partial \phi}\right) \quad (2)$$

where a is the radius of Earth. Finally, the vertical mass flux decomposed into zonal and meridional components of the circulation can be calculated:

$$(m_\lambda, m_\phi) = -(\omega_\lambda \cos \phi / g, \omega_\phi \cos \phi / g) \quad (3)$$

In this study, only the local Hadley overturning circulation is presented and can be computed by averaging the meridional components of the circulation zonally, in this case for the southern Africa sector 10° to 40°E. European Centre for Medium-Range Weather Forecasts interim reanalysis (ERA-I; Dee et al., 2011) derived vertical velocity is used for an estimate of observed regional circulation.

Accurate representation of deep tropical convection and the associated vertical mass flux over southern Africa is likely to be necessary for accurate simulation of the subtropical climate. Figure 3a shows that LAM25, like the

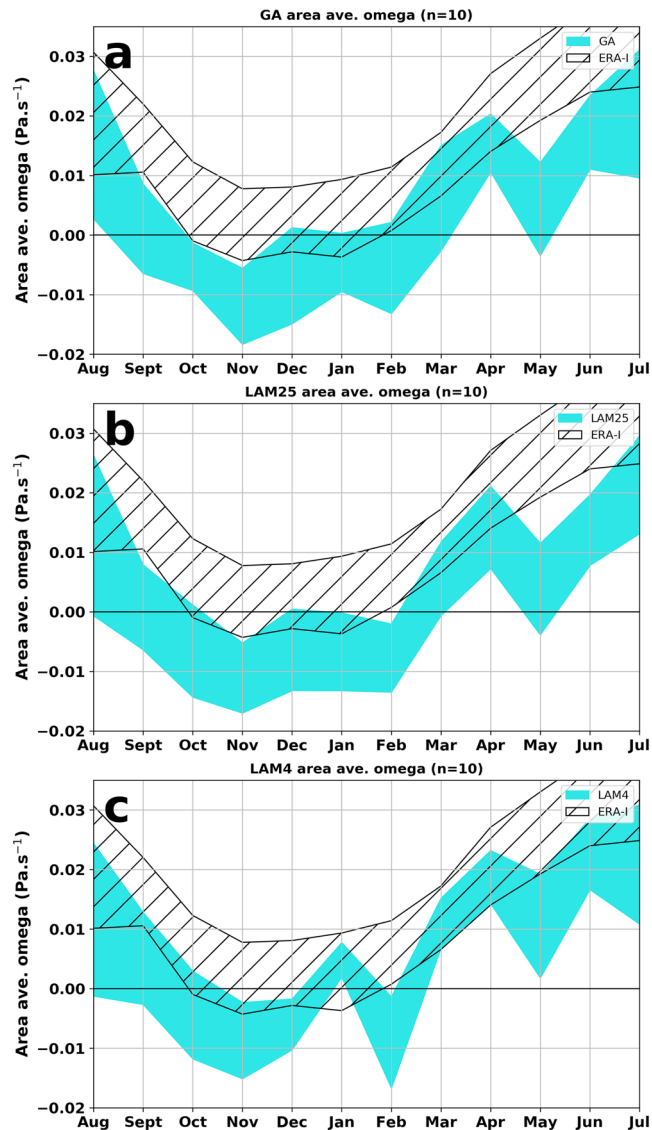


Figure 5. The monthly interquartile range in domain-averaged ($15^{\circ}\text{E}-40^{\circ}\text{E}$, $20^{\circ}\text{E}-35^{\circ}\text{S}$) subsidence at 500-hPa pressure level as simulated by (a) GA N512, (b) regional LAM25, and (c) regional convective-permitting LAM4. ERAI interquartile range is shown in black hatching and model-simulated interquartile range shown in light blue. GA = Global Atmosphere; LAM = limited area model; ERAI = ERA-Interim.

global simulation (not shown), produces a strong overturning circulation into the winter hemisphere (Northern Hemisphere) in the November–January mean. There is however, negligible overturning in the Southern Hemisphere.

LAM4, however, simulates more substantial southward overturning (Figure 3b) with poleward flow above 300 hPa. The upper-tropospheric subsidence between 20° and 30°S is twice the magnitude of that in the LAM25 simulation. The origin of this stronger southward overturning is related to the substantial increase in total upward mass flux in the tropics simulated by LAM4 (Figure 3). This increased tropical mass flux is reflected in the 10–20% rainfall bias increase in a narrow tropical band noted in section 3 (Figure 3f).

Reanalyzed observations of this overturning circulation are stronger than the LAM4 simulation, with downward mass flux up to $1 \times 10^3 \text{ kg}\cdot\text{m}^{-2}\cdot\text{s}^{-1}$ extending to 600 hPa (not shown) over subtropical southern Africa. In LAM4, this magnitude of mass flux reaches 500 hPa, whereas in the parametrized convection regional model (and global, not shown), such subsidence barely reaches 400 hPa. The implications of these summer hemisphere local Hadley cell differences between LAM25 and LAM4 are discussed next.

5. Stronger Forcing of Subtropical Westerlies and Subtropical Subsidence

The stronger overturning circulation simulated by the LAM4 simulation has two likely outcomes in the subtropics: stronger local forcing of the subtropical westerlies and suppression of midlevel vertical motion. Hart et al. (2018) demonstrated, with reanalysis data, that the presence of a subtropical jet maxima, distinguishable from the midlatitude eddy-driven jet, was associated with higher monthly TE cloud band frequency than months without such a distinct subtropical jet. A strongly distinct upper-level subtropical jet indicates a situation in which there will be lower meridional shear in the zonal winds across the subtropics than when the subtropics have weak upper-level westerlies or even easterlies. The meridional shear is a critical variable for determining the propagation and zonal deformation of the upper-level westerly waves, which are fundamental to TE cloud band formation (Hart et al., 2010). We diagnose this subtropical shear by computing the difference between the zonal mean wind in a 20° – 25° S band and a 30° – 35° S band, across the same longitude sector, 10° to 40° E, as used in Figure 3. This subtropical shear is presented in Figure 4.

Figure 4 demonstrates that the weak overturning in the global model and LAM25 results in larger negative values of subtropical shear during the summer months than observed in ERAI. Subtropical shear in LAM4 is smaller and in close agreement to ERAI throughout the early and midsummer months, as expected from stronger overturning and the associated stronger forcing of subtropical westerlies. This weaker shear supports the more faithful simulation of the annual cloud band cycle (Figure 1), particularly through the most active cloud band months of November to March. We speculate that the spurious winter cloud band events that the parametrized models simulate are unrelated to shear and are associated with processes not diagnosed here.

The parametrized models simulate too much subtropical rainfall, which suggests that the regional environment is too frequently favorable for convection. Figure 5 shows the interquartile range of area-averaged 500-hPa vertical velocity for each model simulation with the ERAI interquartile range hatched for reference. All three model simulations are dominated by ascent in contrast to descent computed in ERAI, during October to February. However, the LAM4 simulation has close to half the magnitude of ascent in the parametrized convection simulations. The reduced area average ascent is consistent with diagnosed monthly mean profile instabilities; LAM4 exhibits more stable profiles than LAM25 and global simulations (not shown). A more stable atmosphere, with reduced ascent bias, is an expected outcome of the stronger upper-level subsidence as shown by the mass flux in Figure 3 and explains much of the reduction in wet bias over the region (Figure 2).

6. Conclusions

A 10-year pan-African convection-permitting climate simulation shows stronger meridional overturning into subtropical southern African when compared to climate simulations run with the same dynamical core but configured at a lower resolution with parametrized convection. The near-doubling of LAM4 overturning compared to LAM25 brings the convective-permitting model simulation closer to the observed overturning magnitude estimated by reanalysis in terms of both magnitude and vertical extent of subtropical descending mass flux. The convection-permitting simulation of the regional climate halves the wet bias in rainfall and accurately captures the annual cycle of TE cloud bands, which are fundamental to the regional hydroclimate and extremes.

These improvements happen for two related outcomes of the strengthened local Hadley cell: stronger tropical forcing of a local subtropical jet and stronger suppression of subtropical convection by upper-level subsidence. The more realistic seasonality in the forcing of the local subtropical westerlies supports a better annual cycle of TE cloud band development. The enhanced upper-level subsidence suppresses subtropical convective environments, which accounts for the reduction of the wet rainfall bias during October–January. While not studied here, the upper-level subsidence indicates a more developed midlevel Botswana High (Reason, 2016), and the convective-permitting simulation acts to reduce a bias in midlevel subsidence common across CMIP5 models (Munday & Washington, 2017).

These results add weight to the hypothesis that convective heating over tropical Africa plays a key role in the forcing of a local subtropical jet, and by implication TE cloud band likelihood, as posited in Hart et al. (2018). These experiments show that, for subtropical southern Africa, a large portion of climate model error in the region is likely associated with errors in the representation of the deep convection over tropical Africa. Furthermore, even *high-resolution* 25-km global and regional atmosphere climate simulations maintain problematic biases, and the biggest improvement comes from turning off convective parametrization. However,

at the other extreme, Tozuka et al. (2014) demonstrated that, over southern Africa, the choice of convection scheme in a global model could actually enhance the upper-level suppression of subtropical convection to the extent of inducing a dry bias and suppression of TE cloud bands in early summer. Such a simulation error indicates too much local overturning. Until such a time as long-running global climate models can be run at convective-permitting resolutions, convective parametrization development should include close attention to total vertical mass flux, particularly in the tropics. Fortunately, the results presented here demonstrate that much can be gained from long-running convective-permitting regional climate models, which are already computationally feasible.

This study has demonstrated that explicit representation of convection can substantially improve simulated regional circulation in the subtropics. Better representation of local orography, surface characteristics, and subtropical convection in convective-permitting models may result in the improved simulation of subtropical regional climates; however, we have demonstrated that substantial improvements are related to the representation of tropical convection and the associated mass flux into the subtropics. We recommend that regional convective-permitting simulations are pursued with domains large enough to include proximal tropical convection hot spots. Our results suggest this is necessary in order to capture the salient forcing of subtropical regional climates and thereby extract the maximum value from regional climate simulations.

Acknowledgments

This work was carried out under the Future Climate for Africa UMFULA project, with financial support from the U.K. Natural Environment Research Council (NERC), NE/M020207/1 (N. C. G. H. and R. W.); IMPALA project NE/M017214/1 (R. A. S.); and the U.K. Government's Department for International Development (DfID). We thank Malcolm Roberts for running the N512-resolution AMIP global simulation. We are grateful to ECMWF for the provision of the ERA-Interim data set and to NOAA/OAR/ESRL PSD, Boulder, Colorado, for providing the interpolated OLR data, from their website (<http://www.esrl.noaa.gov/psd/>). The metbot analysis code is available at <https://github.com/hart-ncg> and on request from N. C. G. H. Derived data used in figure production are available on request.

References

- Brown, A., Milton, S., Cullen, M., Golding, B., Mitchell, J., & Shelly, A. (2012). Unified modeling and prediction of weather and climate: A 25-year journey. *Bulletin of the American Meteorological Society*, *93*, 1865–1877. <https://doi.org/10.1175/BAMS-D-12-00018.1>
- Dee, D. P., Uppala, S. M., Simmons, A. J., Berrisford, P., Poli, P., Kobayashi, S., et al. (2011). The ERA-Interim reanalysis: Configuration and performance of the data assimilation system. *Quarterly Journal of the Royal Meteorological Society*, *137*, 553–597.
- Harrison, M. S. J. (1984). A generalized classification of South African rain-bearing synoptic systems. *Journal of Climatology*, *4*, 547–560.
- Hart, N. C. G., Reason, C. J. C., & Fauchereau, N. (2010). Tropical-extratropical interactions over southern Africa: Three cases of heavy summer season rainfall. *Monthly Weather Review*, *138*, 2608–2623. <https://doi.org/10.1175/2010MWR3070.1>
- Hart, N. C. G., Reason, C. J. C., & Fauchereau, N. (2012). Building a tropical-extratropical cloud band metbot. *Monthly Weather Review*, *140*, 4005–4016. <https://doi.org/10.1175/MWR-D-12-00127.1>
- Hart, N. C. G., Reason, C. J. C., & Fauchereau, N. (2013). Cloud bands over southern Africa: Seasonality, contribution to rainfall variability and modulation by the MJO. *Climate Dynamics*, *41*, 1199–1212. <https://doi.org/10.1007/s00382-012-1589-4>
- Hart, N. C. G., Washington, R., & Reason, C. J. C. (2018). On the likelihood of tropical-extratropical cloud bands in the south Indian convergence zone during ENSO events. *Journal of Climate*, *31*, 2797–2817. <https://doi.org/10.1175/JCLI-D-17-0221.1>
- Huffman, G., Adler, R., Bolvin, D., Gu, G., Nelkin, E., Bowman, K., et al. (2007). The TRMM multi-satellite precipitation analysis: Quasi-global, multi-year, combined-sensor precipitation estimates at fine scale. *Journal of Hydrometeorology*, *8*, 38–55.
- James, R., Washington, R., Abiodun, B., Kay, G., Mutemi, J., Pokam, W., et al. (2018). Evaluating climate models with an African lens. *Bulletin of the American Meteorological Society*, *99*, 313–336. <https://doi.org/10.1175/BAMS-D-16-0090.1>
- Kendon, E. J., Ban, N., Roberts, N. M., Fowler, H. J., Roberts, M. J., Chan, S. C., et al. (2017). Do convection-permitting regional climate models improve projections of future precipitation change? *Bulletin of the American Meteorological Society*, *98*, 79–93. <https://doi.org/10.1175/BAMS-D-15-0004.1>
- Kendon, E. J., Roberts, N. M., Fowler, H. J., Roberts, M. J., Chan, S. C., & Senior, C. A. (2014). Heavier summer downpours with climate change revealed by weather forecast resolution model. *Nature Climate Change*, *4*, 570–576. <https://doi.org/10.1038/nclimate2258>
- Lazenby, M. J., Todd, M. C., & Wang, Y. (2016). Climate model simulation of the South Indian Ocean convergence zone: Mean state and variability. *Climate Research*, *68*, 59–71. <https://doi.org/10.3354/cr01382>
- Lee, H.-T. (2014). Climate algorithm theoretical basis document (C-ATBD): Outgoing longwave radiation (OLR)-daily (Tech. Rep.) (46 pp.). Boulder, CO: CDRP-ATBD-0526, NOAA's Climate Data Record (CDR) Program.
- Munday, C., & Washington, R. (2017). Circulation controls on southern African precipitation in coupled models: The role of the Angola Low. *Journal of Geophysical Research: Atmospheres*, *122*, 861–877. <https://doi.org/10.1002/2016JD025736>
- Prein, A. F., Liu, C., Ikeda, K., Bullock, R., Rasmussen, R. M., Holland, G., & Clark, M. (2017a). Simulating North American mesoscale convective systems with a convection-permitting climate model. *Climate Dynamics*. <https://doi.org/10.1007/s00382-017-3993-2>
- Prein, A. F., Liu, C., Ikeda, K., Trier, S. B., Rasmussen, R. M., Holland, G., & Clark, M. (2017b). Increased rainfall volume from future convective storms in the US. *Nature Climatic Change*, *7*, 880–884.
- Reason, C. J. C. (2016). The Bolivian, Botswana, and Bilybara Highs and Southern Hemisphere drought/floods. *Geophysical Research Letters*, *43*, 1280–1286. <https://doi.org/10.1002/2015GL067228>
- Sardeshmukh, P. D., & Hoskins, B. J. (1988). The generation of global rotational flow by steady idealized tropical divergence. *Journal of the Atmospheric Sciences*, *45*, 1228–1251. [https://doi.org/10.1175/1520-0469\(1988\)045<1228:TGOGRF>2.0.CO;2](https://doi.org/10.1175/1520-0469(1988)045<1228:TGOGRF>2.0.CO;2)
- Schwendike, J., Govekar, P., Reeder, M. J., Wardle, R., Berry, G. J., & Jakob, C. (2014). Local partitioning of the overturning circulation in the tropics and the connection to the Hadley and Walker circulations. *Journal of Geophysical Research: Atmospheres*, *119*, 1322–1339. <https://doi.org/10.1002/2013JD020742>
- Stratton, R. A., Senior, C. A., Vosper, S. B., Folwell, S. S., Boutle, I. A., Earnshaw, P. D., et al. (2018). A pan-African convection-permitting regional climate simulation with the Met Office Unified Model: CP4-Africa. *Journal of Climate*, *31*, 3485–3508. <https://doi.org/10.1175/JCLI-D-17-0503.1>
- Tozuka, T., Abiodun, B. J., & Engelbrecht, F. A. (2014). Impacts of convection schemes on simulating tropical-temperature troughs over southern Africa. *Climate Dynamics*, *42*, 433–451. <https://doi.org/10.1007/s00382-013-1738-4>
- Washington, R., & Todd, M. (1999). Tropical-temperate links in southern Africa and southwest Indian Ocean satellite-derived daily rainfall. *International Journal of Climatology*, *19*, 1601–1616.